

AGN outflows as neutrino sources: an observational test

P. Padovani^{1,2★}, A. Turcati³, E. Resconi³

¹*European Southern Observatory, Karl-Schwarzschild-Str. 2, D-85748 Garching bei München, Germany*

²*Associated to INAF - Osservatorio Astronomico di Roma, via Frascati 33, I-00040 Monteporzio Catone, Italy*

³*Technische Universität München, Physik-Department, James-Frank-Str. 1, D-85748 Garching bei München, Germany*

Accepted XXX. Received YYY; in original form ZZZ

ABSTRACT

We test the recently proposed idea that outflows associated with Active Galactic Nuclei (AGN) could be neutrino emitters in two complementary ways. First, we cross-correlate a list of 94 “bona fide” AGN outflows with the most complete and updated repository of IceCube neutrinos currently publicly available, assembled by us for this purpose. It turns out that AGN with outflows matched to an IceCube neutrino have outflow and kinetic energy rates, and bolometric powers larger than those of AGN with outflows not matched to neutrinos. Second, we carry out a statistical analysis on a catalogue of [O III] λ 5007 line profiles using a sample of 23,264 AGN at $z < 0.4$, a sub-sample of which includes mostly possible outflows sources. We find no significant evidence of an association between the AGN and the IceCube events, although we get the smallest p-values (~ 6 and 18 per cent respectively, pre-trial) for relatively high velocities and luminosities. Our results are consistent with a scenario where AGN outflows are neutrino emitters but at present do not provide a significant signal. This can be tested with better statistics and source stacking. A predominant role of AGN outflows in explaining the IceCube data appears in any case to be ruled out.

Key words: neutrinos — radiation mechanisms: non-thermal — galaxies: active — ISM: kinematics and dynamics

1 INTRODUCTION

The IceCube South Pole Neutrino Observatory¹ has reported in the past few years the first observations of high-energy astrophysical neutrinos² (Aartsen et al. 2013; IceCube Collaboration 2013, 2014, 2015a). Recently, it has confirmed and strengthened these observations by publishing a sample of 82 high-energy starting events (HESE) collected over six years and with a deposited energy up to 2 PeV (IceCube Collaboration 2017b), which are inconsistent with the hypothesis of purely terrestrial origin with very high significance ($> 6.5\sigma$).

These HESE cover the whole sky and are mostly cascade-like events, which can only be reconstructed with a spatial resolution in the tens of degrees. There is also a complementary sample of through-going charged current ν_μ from the northern sky studied over a period of eight years (Aartsen et al. 2015; IceCube Collaboration 2015b; Aartsen et al. 2016; IceCube Collaboration 2017a). These are almost

all track-like, meaning that their positions are known typically within one degree or less.

Where are these neutrinos coming from? Since their sky distribution is isotropic (e.g., IceCube Collaboration 2017b) most of them need to have an extragalactic origin, although a minor Galactic component cannot be excluded. Many different scenarios for the astrophysical counterparts of IceCube neutrinos have been put forward, including blazars, star-forming galaxies, γ -ray bursts, galaxy clusters, and high-energy Galactic sources (see, e.g. Ahlers & Halzen 2015, and references therein, for a comprehensive discussion). Of these, blazars are so far the most supported by the data.

Blazars are AGN (see Padovani et al. 2017, for a recent review) having a jet at a small angle with respect to the line of sight. The jet is highly relativistic and contains particles moving in a magnetic field emitting non-thermal radiation over the whole electromagnetic spectrum (Urry & Padovani 1995; Padovani et al. 2017). Blazars come in two main flavours: BL Lacertae objects (BL Lacs) and flat-spectrum radio quasars (FSRQ). These differ mostly in their optical spectra, with the latter displaying strong, broad, quasar-like emission lines and the former instead having optical spectra with at most weak emission lines, sometimes

★ E-mail: ppadovan@eso.org

¹ <http://icecube.wisc.edu>

² In this paper neutrino means both neutrino and antineutrino.

exhibiting absorption features, and in many cases totally featureless. The possibility that blazars could be high-energy neutrino sources goes back to long before the IceCube detections and has since been investigated in a number of papers (e.g., Mannheim 1995; Halzen & Zas 1997; Mücke et al. 2003; Padovani & Resconi 2014; Petropoulou et al. 2015; Tavecchio & Ghisellini 2015).

In particular, Padovani et al. (2016) have correlated the second catalogue of hard *Fermi*-LAT sources (2FHL) ($E > 50$ GeV, 360 sources of various types, mainly blazars, Ackermann et al. 2016), and two other catalogues with the publicly available high-energy neutrino sample detected by IceCube (including only events with energy and median angular error ≥ 60 TeV and $\leq 20^\circ$ respectively and covering the first four years of HESE data). The chance probability scanning over the γ -ray flux was 0.4 per cent, which becomes 1.4 per cent (2.2σ) by evaluating the impact of the trials (Resconi et al. 2017, see also Sect. 3.2.1). This applies only to high-energy peaked (HBL) blazars (sources with the peak of the synchrotron emission $\nu_{\text{peak}}^S > 10^{15}$ Hz; Padovani & Giommi 1995) and appears to be strongly dependent on γ -ray flux. The fraction of the IceCube signal explained by HBL is however only $\sim 10 - 20$ per cent, which agrees with the results of Padovani et al. (2015), who have calculated the cumulative neutrino emission from BL Lacs. Within the so-called *blazar simplified view* (e.g. Giommi et al. 2012) and by adding a hadronic component from Petropoulou et al. (2015) for neutrino production, BL Lacs as a class were in fact shown to be able to explain the neutrino background seen by IceCube above ~ 0.5 PeV while only contributing on average ~ 10 per cent at lower energies. This is consistent with Aartsen et al. (2017), who by searching for cumulative neutrino emission from blazars in the second *Fermi*-LAT AGN (2LAC) catalogue, have constrained the maximum contribution of 2LAC blazars to the observed astrophysical neutrino flux to < 27 per cent. Similar results have been obtained by IceCube Collaboration (2017c) using three more recent catalogues, a larger IceCube sample, and a range of γ -ray spectral shapes.

In what is so far the most significant result³ Resconi et al. (2017) have presented a strong hint of a connection between HBL, IceCube neutrinos, and ultra high-energy cosmic rays (UHECRs; $E \geq 52 \times 10^{18}$ eV) with a probability ~ 0.18 per cent (2.9σ) after compensation for all the considered trials. Even in this case, HBL can account only for ≈ 10 per cent of the UHECR signal.

It is interesting to note that none of the possible neutrino counterparts in Padovani et al. (2016) and Resconi et al. (2017) are tracks, as they are all cascade-like. And indeed Palladino & Vissani (2017) did not find a significant correlation between 2FHL BL Lacs and 29 IceCube tracks. This indicates that by using tracks we are still not sensitive to

³ Emig, Lunardini, & Windhorst (2015) found a hint (p-value ~ 0.3 per cent) of an association between the 37 IceCube neutrinos detected in the first three years of operation and a set of γ -ray detected starburst galaxies and star-forming regions in the Galactic neighbourhood. However, no trial correction was done (so the p-value is only a lower limit) and most of their sources appear to fail the “energetic” test suggested by Padovani & Resconi (2014), i.e. their extrapolated γ -ray spectra fall well below the neutrino flux of the corresponding IceCube event.

the HBL neutrino signal, as also expected from the fact that tracks trace only about 1/6 of the astrophysical signal under the assumption of a flavour ratio $\nu_e : \nu_\mu : \nu_\tau = 1 : 1 : 1$ (as pointed out by Padovani et al. 2016). Very recently, however, Lucarelli et al. (2017a) have found a transient γ -ray (> 100 MeV) source positionally coincident with an IceCube track with a post-trial significance $\sim 4\sigma$ and possibly associated with an HBL. Moreover, γ -ray emission from *Fermi*, AGILE, and MAGIC (Tanaka, Buson, & Kocevski 2017; Lucarelli et al. 2017b; Mirzoyan 2017) has been detected from a BL Lac (with ν_{peak}^S close to HBL values) inside the error region of an IceCube track (Kopper & Blaufuss 2017; see also Padovani et al., in prep.). These could be the *first* observed electromagnetic counterparts of IceCube neutrinos.

In summary, while the evidence for HBL as neutrino emitters is getting stronger, it is also clear that these sources cannot explain the whole IceCube signal, which leaves room for other astrophysical components.

The purpose of this paper is to consider a new, possible class of neutrino emitters: AGN outflows. Many AGN show evidence for large-scale outflows of matter driven by the central black hole (see, e.g., Harrison 2017; Fiore et al. 2017, and references therein). These can reach semi-relativistic speeds of up to $\sim 50,000$ km s⁻¹ that can drive a shock that accelerates and sweeps up matter (e.g., King & Pounds 2015). The protons accelerated by these shocks can generate γ -ray emission via collisions with protons in the interstellar medium by producing neutral and charged pions. The former decay into two γ -rays ($\pi^0 \rightarrow \gamma + \gamma$) while the latter decay into secondary electrons, positrons, and neutrinos. Wang & Loeb (2016) and Lamastra et al. (2017) have shown that, using two different approaches and assuming that *all* AGN have outflows, the neutrino emission from such outflows could explain the *whole* IceCube signal. Liu et al. (2018), on the other hand, by including adiabatic losses not taken into account by other studies, have ruled out a dominant contribution to the IceCube flux from AGN outflows, which might contribute only at the ≈ 20 per cent level. We stress that AGN outflows are not simply (yet) another feature related to the central black hole but also play a major role on galaxy scales through the so-called AGN feedback (e.g., Fabian 2012, for a review). This happens through the interaction between the accretion-related radiation produced by the black hole and gas in the host galaxy, which might sweep the galaxy bulge clean of interstellar gas, put an end to star formation and, through lack of fuel, also starve to death the AGN. Such a feedback mechanism explains in a natural way the observed scaling relationship between the central black hole and the host galaxy bulge mass.

The AGN outflow neutrino scenario has not been tested quantitatively so far. This is what we plan to do in this paper by taking advantage of the larger neutrino samples recently provided by the IceCube Collaboration (including both cascades and tracks) and using two complementary approaches. Namely we want to: (1) investigate the possible link between IceCube neutrinos and a very comprehensive list of “bona fide” AGN displaying outflows; (2) study the possible connection between IceCube neutrinos and a large catalogue of AGN with optical spectral line information, which potentially includes sources exhibiting outflows.

Table 1: IceCube events

IceCube ID	Dep. Energy (TeV)	RA (2000)	Dec (2000)	Median Angular Error (deg)	Topology
HES3	75.7	08 31 36	-31 12 00	1.4	Track
HES4	159.1	11 17 59	-51 12 00	7.1	Cascade
HES5	68.7	07 22 23	-00 24 00	1.2	Track
HES9	60.8	10 05 11	+33 36 00	16.5	Cascade
HES10	93.5	00 19 59	-29 24 00	8.1	Cascade
HES11	85.0	10 21 12	-08 54 00	16.7	Cascade
HES12	100.2	19 44 24	-52 48 00	9.8	Cascade
HES13	243.1	04 31 36	+40 18 00	1.2	Track
HES14	1001.4	17 42 23	-27 54 00	13.2	Cascade
HES17	192.2	16 29 35	+14 30 00	11.6	Cascade
HES19	68.8	05 07 35	-59 42 00	9.7	Cascade
HES20	1097.7	02 33 11	-67 12 00	10.7	Cascade
HES22	211.2	19 34 48	-22 06 00	12.1	Cascade
HES23	79.1	13 54 47	-13 12 00	1.9	Track
HES26	202.1	09 33 35	+22 42 00	11.8	Cascade
HES30	123.8	06 52 47	-82 42 00	8.0	Cascade
HES33	370.2	19 30 00	+07 48 00	13.5	Cascade
HES35	1928.0	13 53 35	-55 48 00	15.9	Cascade
HES38	193.0	06 13 11	+14 00 00	1.2	Track
HES39	97.5	07 04 47	-17 54 00	14.2	Cascade
HES40	151.4	09 35 35	-48 30 00	11.7	Cascade
HES41	84.2	04 24 23	+03 18 00	11.1	Cascade
HES44	81.4	22 26 48	+00 00 00	1.2	Track
HES45	413.6	14 35 59	-86 18 00	1.2	Track
HES46	152.0	10 01 59	-22 18 00	7.6	Cascade
HES47	71.5	13 57 35	+67 24 00	1.2	Track
HES48	100.8	14 11 59	-33 12 00	8.1	Cascade
HES51	63.7	05 54 23	+54 00 00	6.5	Cascade
HES52	152.2	16 51 11	-54 00 00	7.8	Cascade
HES56	104.2	18 41 59	-50 06 00	6.5	Cascade
HES57	132.1	08 11 59	-42 12 00	14.4	Cascade
HES59	124.6	04 13 11	-03 54 00	8.8	Cascade
HES60	93.0	02 10 48	-37 54 00	13.3	Cascade
HES62	75.8	12 31 35	+13 18 00	1.3	Track
HES63	97.4	10 39 59	+06 30 00	1.2	Track
HES64	70.8	09 37 59	-27 18 00	10.6	Cascade
HES66	84.2	08 34 47	+38 18 00	18.3	Cascade
HES67	165.7	22 22 47	+03 00 00	7.0	Cascade
HES70	98.8	06 15 35	-33 30 00	12.3	Cascade
HES71	73.5	05 22 47	-20 48 00	1.2	Track
HES74	71.3	22 44 00	-00 54 00	12.7	Cascade
HES75	164.0	17 15 59	+70 30 00	13.1	Cascade
HES76	126.3	16 00 47	-00 24 00	1.2	Track
HES79	158.2	01 38 23	-11 06 00	14.6	Cascade
HES80	85.6	09 46 24	-03 36 00	16.1	Cascade
HES81	151.8	03 00 00	-79 24 00	13.5	Cascade
HES82	159.3	16 03 35	+09 24 00	1.2	Track
AHES1	18883.62*	16 02 16	+09 18 00	0.60 [†]	Track
AHES2	15814.74*	14 20 26	-00 30 00	1.23 [†]	Track
AHES3	10431.02*	13 17 14	-32 00 00	1.49 [†]	Track
AHES4	7546.05*	02 43 19	+12 36 00	0.88 [†]	Track
AHES5	8858.64*	20 20 35	-26 36 00	0.47 [†]	Track
AHES6	8685.07*	14 47 11	-26 00 00	2.40 [†]	Track
AHES7	13906.14*	10 51 26	-15 23 59	1.94 [†]	Track
DIF1	480	01 58 20	+01 13 47	0.31 [†]	Track
DIF2	250	19 52 50	+11 44 23	0.45 [†]	Track
DIF3	340	22 59 43	+23 34 47	3.06 [†]	Track

Table 1: IceCube events

IceCube ID	Dep. Energy (TeV)	RA (2000)	Dec (2000)	Median Angular Error (deg)	Topology
DIF4	260	09 24 59	+47 48 00	0.43 [†]	Track
DIF5	230	20 27 50	+21 00 00	2.13 [†]	Track
DIF6	770	16 47 59	+15 12 35	10.73 [†]	Track
DIF7	460	17 45 09	+13 24 00	0.54 [†]	Track
DIF8	660	22 04 19	+11 05 23	0.55 [†]	Track
DIF9	950	05 55 47	+00 30 00	0.39 [†]	Track
DIF10	520	19 03 48	+03 09 00	1.09 [†]	Track
DIF11	240	20 30 50	+01 01 47	0.37 [†]	Track
DIF12	300	15 40 31	+20 18 00	1.71 [†]	Track
DIF13	210	18 08 52	+35 33 00	0.85 [†]	Track
DIF14	210	21 02 38	+05 17 23	5.21 [†]	Track
DIF15	300	14 51 28	+01 52 11	3.53 [†]	Track
DIF16	660	02 26 36	+19 06 00	1.96 [†]	Track
DIF17	200	13 14 57	+31 57 35	0.96 [†]	Track
DIF18	260	22 00 24	+01 34 12	0.61 [†]	Track
DIF19	210	13 40 26	-02 23 24	0.54 [†]	Track
DIF20	750	11 18 26	+28 02 23	0.85 [†]	Track
DIF22	400	14 59 33	-04 26 23	1.05 [†]	Track
DIF23	390	02 11 45	+10 12 00	0.52 [†]	Track
DIF24	850	19 33 09	+32 49 11	0.56 [†]	Track
DIF25	400	23 17 33	+18 03 00	2.70 [†]	Track
DIF26	340	07 05 02	+01 17 23	1.57 [†]	Track
DIF27	4450	07 22 31	+11 25 12	0.37 [†]	Track
DIF28	210	06 41 55	+04 33 35	1.08 [†]	Track
DIF29	240	06 06 23	+12 10 48	0.40 [†]	Track
DIF30	300	21 41 59	+26 06 00	1.62 [†]	Track
DIF31	380	21 53 35	+06 00 00	0.55 [†]	Track
DIF32	220	08 55 59	+28 00 00	0.45 [†]	Track
DIF33	230	13 10 23	+19 53 59	2.33 [†]	Track
DIF34	740	05 05 11	+12 36 00	0.66 [†]	Track
DIF35	380	01 02 23	+15 36 00	0.53 [†]	Track
EHE1	15814.74*	14 18 09	-00 18 00	0.75	Track
EHE2	—	08 11 11	-00 48 00	0.10	Track
EHE3	100.00	03 06 19	+15 00 00	0.78 [†]	Track
EHE4	120.00	06 33 11	-15 00 00	1.18 [†]	Track
EHE5	120.00	05 09 43	+05 41 59	0.83 [†]	Track
EHE6	230.00	22 39 59	+07 24 00	0.47 [†]	Track

* Deposited energy in photoelectronvolt units.

† 90% C.L. angular uncertainty

Section 2 describes the neutrino and AGN outflow catalogues used in this paper, while Section 3 gives our results, which are interpreted in Section 4. Section 5 summarises our conclusions. We use a Λ CDM cosmology with $H_0 = 70 \text{ km s}^{-1} \text{ Mpc}^{-1}$, $\Omega_m = 0.3$, and $\Omega_\Lambda = 0.7$.

2 THE CATALOGUES

2.1 Neutrino lists

This work is based on the IceCube HESE published by [IceCube Collaboration \(2014, 2015a, 2017b\)](#), which cover the first six years of data (HES in Tab. 1) and the ν_μ selected from a large sample of high-energy through-going muons by applying a 200 TeV deposited energy threshold (DIF) (see [Aartsen et al. 2015; IceCube Collaboration 2015b; Aartsen et al. 2016; IceCube Collaboration 2017a](#)). We also include the neutrinos provided by the Astrophysical Multimessenger Observatory Network (AMON), which include starting (AHES) and extremely high-energy (EHE) events available on-line⁴. Given that these lists are only partially up to date, for these neutrinos we gathered the most recent information by checking the Gamma-ray Coordinates Network (GCN) archive. We have also excluded two events: one which has been retracted and another one, which was missing the angular error.

Following [Padovani & Resconi \(2014\)](#) we made the following two cuts to the HESE list: (1) neutrino energy $E_\nu \geq 60 \text{ TeV}$, to reduce the residual atmospheric background contamination, which might still be produced by muons and atmospheric neutrinos and concentrates in the low-energy part of spectrum (see Fig. 2 in [IceCube Collaboration 2014](#)); (2) median angular error $\leq 20^\circ$, to somewhat limit the number of possible counterparts. The final list includes 47 HESE, 34 through-going ν_μ , 7 AHES, and 6 EHE, for a total of 94 IceCube events. These are listed in Tab. 1, which gives the ID, the deposited energy of the neutrino, the coordinates, the median angular error or 90% uncertainty in degrees, and the event topology.

We stress that, to the best of our knowledge, Tab. 1 is the *only* complete (modulo the two cuts made to the HESE list) and updated repository of IceCube neutrinos currently publicly available.

2.2 AGN outflow catalogues

2.2.1 The AGN outflow list

[Fiore et al. \(2017\)](#) have studied scaling relations between AGN properties, host galaxy properties, and AGN outflows. To do so, they have assembled from the literature observations of 94 distinct AGN with reliable massive outflow detections, for which there was an estimate (or a robust limit) on the physical size of the high velocity gas in the wind. As stressed by the authors their sample is not complete and suffers from strong selection biases, different for the various types of outflows. In particular, most molecular winds and

ultrafast outflows (UFOs) can only be studied locally (typically at $z \lesssim 0.2$), ionised winds are found both at low-redshift and at $z \sim 2 - 3$, while broad absorption line (BAL) sources are at $z \sim 2 - 3$. Their list (see their Tab. B1) is therefore a very comprehensive compilation of AGN outflows but does not represent a well-defined sample with which to do statistical studies. As such, it is therefore fully complementary to the SDSS catalogue, discussed below.

2.2.2 The SDSS catalogue

[Mullaney et al. \(2013\)](#) have presented a catalogue of [O III] $\lambda 5007$ line profiles using a sample of 23,264 AGN at $z < 0.4$ selected from the Sloan Digital Sky Survey (SDSS) DR7 data base. These can be used to determine the kinematics of the kpc-scale emitting gas. Using their data we have computed the [O III] $\lambda 5007$ flux-weighted average full width half-maximum (FWHM):

$$\text{FWHM}_{\text{Avg}} = [(\text{FWHM}_{\text{broad}} F_{\text{broad}})^2 + (\text{FWHM}_{\text{narr}} F_{\text{narr}})^2]^{1/2} \quad (1)$$

where F_{broad} and F_{narr} are the fractional fluxes contained within the two fitted Gaussian components of the [O III] $\lambda 5007$ line, a broad and a narrow one. As discussed by [Mullaney et al. \(2013\)](#) it is better to use the average FWHM rather than a single component (e.g., $\text{FWHM}_{\text{broad}}$) as this also allows inclusion of sources for which the line is satisfactorily fitted by a single Gaussian. We note that $\text{FWHM}_{\text{Avg}} > 500 \text{ km s}^{-1}$ is the typical lower limit generally adopted when selecting targets for follow-up (i.e., with integral field unit [IFU]) spectroscopic studies of AGN outflows (e.g., [Harrison et al. 2014](#)). The [Mullaney et al. \(2013\)](#) catalogue includes 17 per cent of sources above this value and is therefore a very good, well-defined catalogue of AGN with possible outflows to be used for statistical studies. [Harrison et al. \(2014\)](#), in fact, have presented IFU observations of 16 AGN selected from this sample (at the high FWHM_{Avg} and $L_{[\text{O III}]}$ end) and have detected high-velocity outflows on kpc scales in all of them. Power is also another good outflow indicator. For this purpose we use below the *observed* $L_{[\text{O III}]}$ in [Mullaney et al. \(2013\)](#) (and not the *de-reddened* one as this reaches some very large and unphysical values due to the V-band magnitude extinction used).

3 RESULTS

3.1 AGN outflow list

We cross-correlated our neutrino list with the AGN outflow list of [Fiore et al. \(2017\)](#). An outflow counterpart was found within the given angular error for 15/96 neutrino events, all HESE of the cascade type. These correspond to 45 entries, 9 of which were matched to multiple IceCube events for a total of 36 distinct AGN. Our results are shown in Tab. 2, which gives the IceCube ID, the AGN counterpart's name and coordinates, the offset between the reconstructed position of the IceCube event and the AGN one, the source redshift, the outflow type, and the HBL listed as "most probable" matches in [Padovani et al. \(2016\)](#). These are sources, which not only are within the median error radius of an IceCube

⁴ See the lists at https://gcn.gsfc.nasa.gov/amon_hese_events.html and https://gcn.gsfc.nasa.gov/amon_ehe_events.html

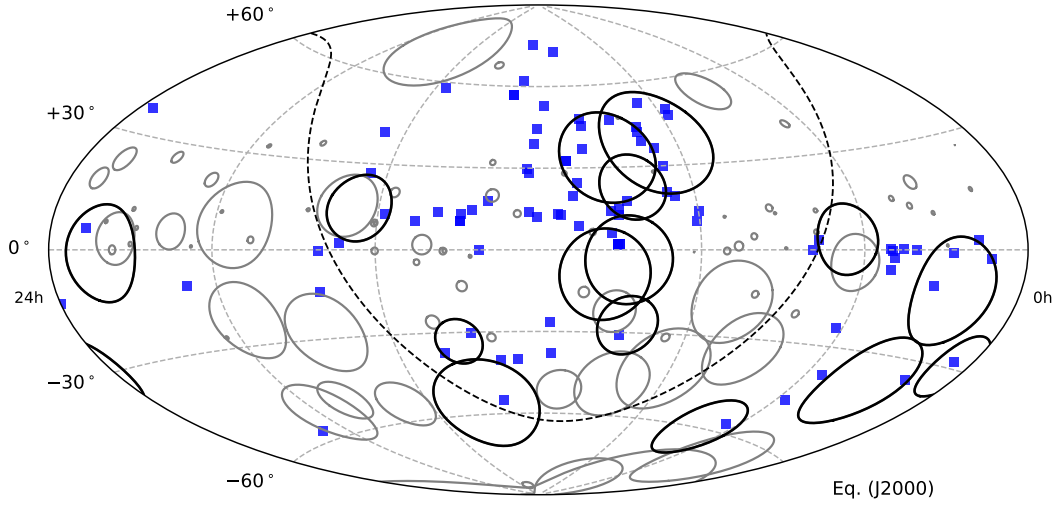


Figure 1. Sky map in equatorial coordinates. Blue squares indicate the AGN with outflows from [Fiore et al. \(2017\)](#), while IceCubes events are represented as circles with radius equal to the angular uncertainty. Black circles indicate neutrinos with a counterpart, grey circles neutrinos without counterparts. The dashed line represents the Galactic plane.

neutrino but for which a simple extrapolation of their γ -ray spectral energy distribution (SED) connects to the neutrino flux.

Fig. 1 shows the positions of the AGN with outflow from [Fiore et al. \(2017\)](#) (blue squares) in equatorial coordinates, while IceCubes events are represented as circles with radius equal to the angular error (with black colour indicating neutrinos with a counterpart and grey neutrinos without). Given the statistical limitations of the AGN outflow list, discussed in Sect. 2.2.1, we cannot test the statistical significance of the neutrino - outflow matches.

[Fiore et al. \(2017\)](#) have presented the basic properties of the AGN with outflows discussed in their paper, deriving also in an homogenous way physical quantities such as the mass outflow rate, \dot{M}_{OF} , and the kinetic energy rate, \dot{E}_{kin} . These are the instantaneous outflow rate of material at the edge of the outflow region (see their eq. B.1 and B.2) and its kinetic power (equal to $\frac{1}{2} \dot{M}_{\text{OF}} v_{\text{max}}^2$, where v_{max} is the outflow maximum velocity). We have looked for possible parameter differences between outflows with and without an IceCube match⁵, finding three: \dot{E}_{kin} , \dot{M}_{OF} , and bolometric power.

Figure 2 shows the distribution of \dot{E}_{kin} for AGN outflows with (solid black line) and without (red dashed line) IceCube counterparts. The two distributions are significantly different ($P \sim 99.6$, ~ 99.7 , and > 99.9 per cent according to a Kolmogorov-Smirnov [KS], Mann-Whitney-Wilcoxon [MWW], and Cramer test respectively⁶), with the outflows with IceCube matches having $\langle \dot{E}_{\text{kin}} \rangle$ larger by a factor ~ 7 than the corresponding value for outflows without IceCube matches.

⁵ The [Fiore et al. \(2017\)](#) list includes multiple entries for some AGN, as outflows were detected in more than one way. We used a list of distinct sources by keeping the entry with the maximum value of \dot{M}_{OF} .

⁶ Although the list is not complete and biased, none of the biases are neutrino related and therefore these tests are meaningful.

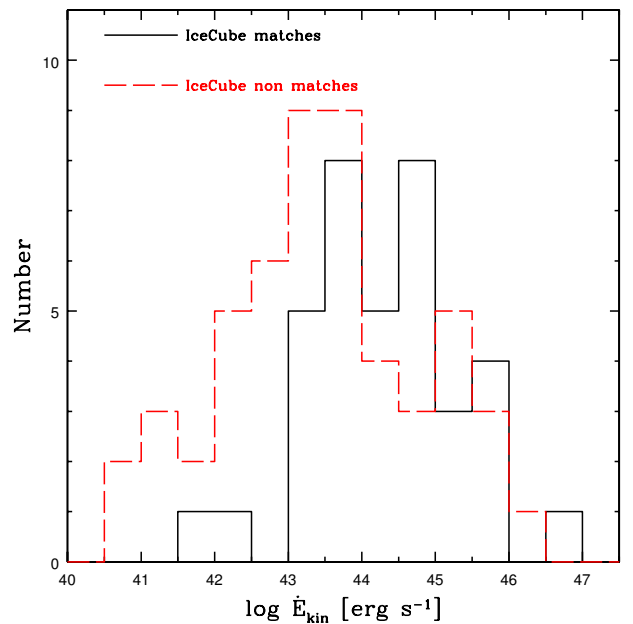


Figure 2. The distribution of the kinetic power for AGN outflows in the list of [Fiore et al. \(2017\)](#) with (solid black line) and without (red dashed line) IceCube counterparts.

Figure 3 shows the distribution of \dot{M}_{OF} for AGN outflows with (solid black line) and without (red dashed line) IceCube counterparts. The two distributions are significantly different ($P \sim 99.6$, ~ 99.6 , and ~ 99.8 per cent according to a KS, MWW, and Cramer test respectively), with the outflows with IceCube matches having $\langle \dot{M}_{\text{OF}} \rangle$ larger by a factor ~ 7 than the corresponding value for outflows without IceCube matches.

Finally, the AGN bolometric power distributions for AGN outflows with and without IceCube counterparts are

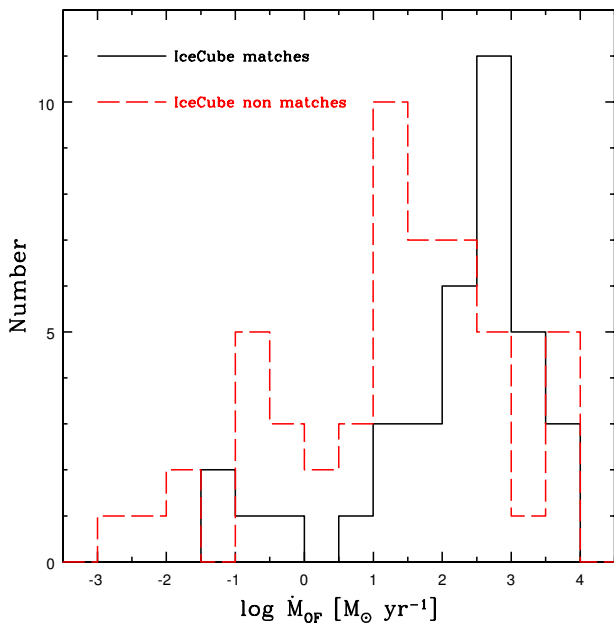


Figure 3. The distribution of the mass outflow rate for AGN outflows in the list of [Fiore et al. \(2017\)](#) with (solid black line) and without (red dashed line) IceCube counterparts.

marginally different ($P \sim 96.2$, ~ 97.6 , and ~ 97.3 per cent according to a KS, MWW, and Cramer test respectively), with the outflows with IceCube matches having bolometric powers *larger* by a factor ~ 4 than the corresponding value for outflows without IceCube matches.

As shown in Tab. 2 four IceCube events have “most probable” matches with HBL, so one could argue that these events should be deleted from this list as it is unlikely they might be associated with AGN outflows. If one does so all differences between AGN outflows with and without IceCube counterparts disappear ($P < 89\%$). In practice, however, this is independent of the choice of the removed IceCube events but it is simply due to the fact that 11 AGN with relatively high values of \dot{E}_{kin} , \dot{M}_{OF} , and bolometric power are moved from one list to the other.

Given this intriguing result, we have followed this up by using a well-defined and complete catalogue, that is the SDSS catalogue, to which we can apply a statistical test to study possible correlations.

3.2 SDSS catalogue

3.2.1 The statistical analysis

To study the possible connection between the IceCube neutrinos and the SDSS catalogue we follow the method of [Padovani et al. \(2016\)](#), which we briefly summarise here.

We use the observable N_V defined as the number of neutrino events with at least one outflow counterpart found within the individual angular uncertainty. We do not only consider the whole catalogue but we additionally scan versus FWHM_{Avg} , $N_V(\text{FWHM}_{\text{Avg}})$, and versus [O III] luminosity, $N_V(L_{[\text{O III}]})$. If only sources with higher outflow velocities or

luminosity are associated with IceCube events, such scans will reveal a deviation from the randomised cases.

The chance probability $P_i(N_V(\text{FWHM}_{\text{Avg}}, i))$, or equivalently $P_i(N_V(L_{[\text{O III}]}, i))$, to observe a given N_V for sources with $\text{FWHM}_{\text{Avg}} \geq \text{FWHM}_{\text{Avg}, i}$ is determined on an ensemble of typically 10^5 randomised maps. As discussed by [Padovani et al. \(2016\)](#) scrambling on the neutrinos right ascension does not conserve the total area sampled by the IceCube error circles, resulting in a biased statistics. To correctly compare the results of a random skymap with real data, in fact, the overlapping area identified by the neutrino angular uncertainty and the portion of the sky covered by the survey must be conserved in each random realisation. This can be achieved by randomising the SDSS coordinates inside the portion of the sky covered by the survey. This area has been approximated using an HEALPix sky pixelisation with a total of 49152 pixels, each covering 0.84 square degrees.

A p-value is then calculated for each of the bins $\text{FWHM}_{\text{Avg}, i}(L_{[\text{O III}]}, i)$, for a total of 8 (11) p-values. When only reporting the lowest p-value observed as a result of the analysis, a trial correction for the “*Look Elsewhere Effect*” is needed (e.g., [Patrignani & Particle Data Group 2016](#)) This stems from a simple fact: in the ideal case of 20 completely independent tests, for example, one will observe one result more significant than $\sim 2\sigma$ simply by chance. The final p-value can in this case be trial corrected by multiplying it by the number of degrees of freedom, i.e. the number of tests. In the cases presented in this paper, however, the bins with a lower value of our scanning parameter include also the bins with a higher value, making our tests not independent. The analytical approximation for the trial correction is then no longer valid, and one needs to study the distribution of the lowest p-value obtained from the randomised cases. A trial corrected p-value can then be calculated as the ratio between the number of randomised trials that produce a best p-value at least as significant as the one given by the data, and the total number of randomised trials.

Fig. 4 shows the positions of the SDSS sources (red dots) in equatorial coordinates, while IceCubes events are represented as circles with radius equal to the angular error (with black colour indicating neutrinos with a counterpart and grey neutrinos without). Given that we perform the randomization on the SDSS positions and due to the large density of SDSS sources, it is apparent that IceCube events with large angular errors (mostly cascades) will almost always give a match (even when the sample gets smaller due to cuts on FWHM_{Avg} or $L_{[\text{O III}]}$: see below) and therefore by default cannot give a signal. We therefore split the sample into cascades and tracks.

3.2.2 Association probabilities

Figure 5 shows the chance probability of association of the SDSS sources with IceCube events for objects having FWHM_{Avg} larger than the value on the x-axis. The dashed red line refers to cascades while the dotted blue line is for tracks; for completeness we also show the results for the full sample (solid orange line). The numbers give the observed (above the points) and average random value (below the points) of N_V . Figure 5 shows the following:

- (i) for all samples the chance probability is strongly de-

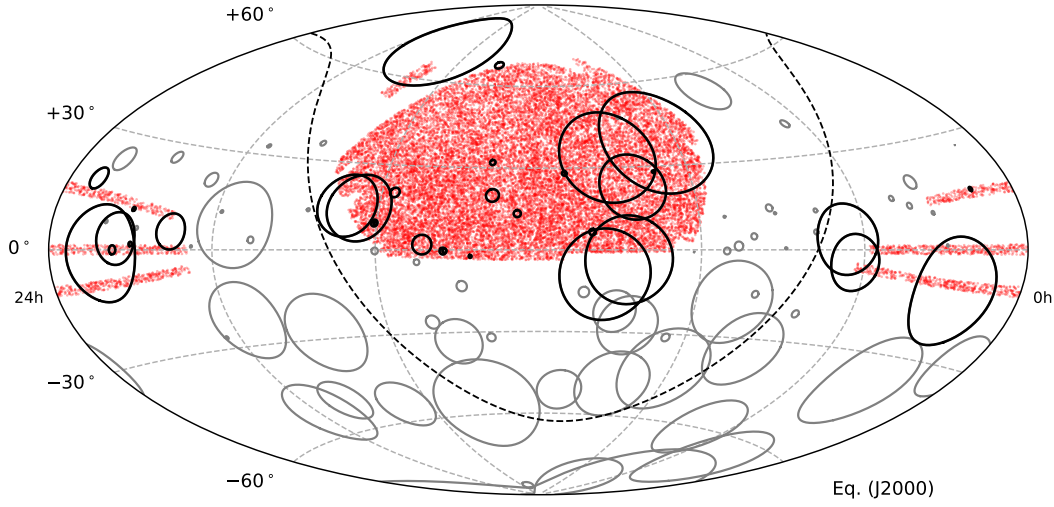


Figure 4. Sky map in equatorial coordinates. Red dots indicate the SDSS objects while IceCubes events are represented as circles with radius equal to the angular error. Black circles indicate neutrinos with a counterpart, grey circles neutrinos without counterparts. The dashed line represents the Galactic plane.

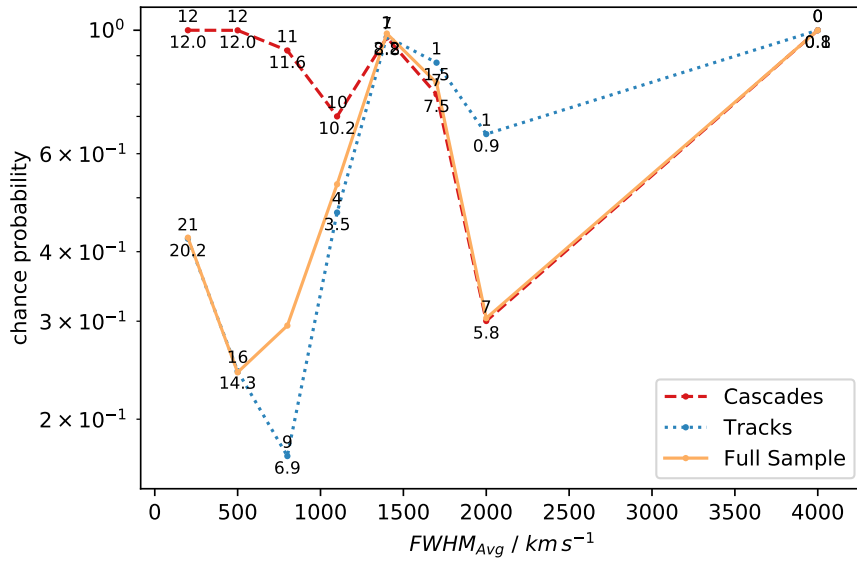


Figure 5. The chance probability of association of SDSS AGN for objects having FWHM_{Avg} larger than the value on the x-axis with all IceCube events (solid orange line), cascades (dashed red line), and tracks (dotted blue line). The numbers give the observed (above the points) and average random values (below the points) of N_{γ} . A p-value ~ 17 per cent is reached for $\text{FWHM}_{\text{Avg}} \gtrsim 800 \text{ km s}^{-1}$ for tracks.

pendent on the proxy for outflow velocity. We attribute the turn-over in p-value at very large velocities to small number statistics;

(ii) a p-value ~ 17 per cent is reached for $\text{FWHM}_{\text{Avg}} \gtrsim 800 \text{ km s}^{-1}$ for tracks. This becomes ~ 48 per cent once the trial correction is applied;

(iii) a p-value ~ 30 per cent is reached for $\text{FWHM}_{\text{Avg}} \gtrsim 2,000 \text{ km s}^{-1}$ for cascades. This becomes ~ 60 per cent once the trial correction is applied. As discussed above, we do not expect a signal for cascades due to the large density of SDSS sources;

(iv) at the FWHM_{Avg} at which the p-value for tracks is

minimum N_{γ} is 9, while the average value from the randomisation is 6.9. Even if we interpreted this excess of ≈ 2 IceCube tracks as “real”, this would imply a contribution to the IceCube signal from possible AGN outflows only at the ~ 6 per cent level, as there are 33 IceCube events in the survey area;

(v) for the same FWHM_{Avg} the number of SDSS sources with a neutrino counterpart is 26, while the whole “parent” SDSS sample includes 747 sources;

(vi) the p-values for the full sample are, as expected, in between those for cascades and tracks.

If we split the tracks even further we get a p-value ~ 6

Table 2. AGN with outflows within one median angular error radius from the positions of the IceCube neutrinos.

ID	Name	RA (2000)	DEC (2000)	offset (deg)	z	outflow type	Other “most probable” matches ^a
HES9	I08572+3915	09 00 25.4	+39 03 54	14.1	0.05835	molecular & ionised	MKN 421, 1ES 1011+496
HES9	I10565+2448	10 59 18.1	+24 32 34	14.9	0.04311	molecular & ionised	” ”
HES9	I11119+3257	11 14 38.9	+32 41 33	14.5	0.189	molecular & UFO	” ”
HES9	SDSSJ0900	09 00 33.5	+42 15 47	15.4	3.297	ionised	” ”
HES9	SMMJ0943	09 43 04.1	+47 00 16	14.0	3.351	ionised	” ”
HES9	SDSSJ1039	10 39 27.2	+45 12 15	13.3	0.579	ionised	” ”
HES9	SDSSJ1040	10 40 14.4	+47 45 55	15.6	0.486	ionised	” ”
HES9	QSO1044	10 44 59.6	+36 56 05	8.8	0.7	BAL	” ”
HES10	2QZJ0028	00 28 30.4	-28 17 06	2.2	2.401	ionised	H 2356-309
HES11	SDSSJ10100	10 10 43.4	+06 12 01	15.3	0.0984	ionised	
HES11	COS11363	10 00 28.7	+02 17 45	12.3	2.1	ionised	
HES11	XID2028	10 02 11.3	+01 37 07	11.5	1.593	ionised	
HES11	XID5321	10 03 08.8	+02 09 04	11.9	1.47	ionised	
HES11	XID5395	10 02 58.4	+02 10 14	12.0	1.472	ionised	
HES11	MIRO20581	10 00 00.6	+02 15 31	12.3	2.45	ionised	
HES17	SDSSJ1549	15 49 38.7	+12 45 09	9.9	2.367	ionised	PG 1553+113
HES19	1H0419-577	04 26 00.7	-57 12 01	6.0	0.104	UFO	
HES26	SDSSJ0945	09 45 21.3	+17 37 53	5.8	0.1283	ionised	
HES26	SDSSJ0958	09 58 16.9	+14 39 24	9.9	0.1092	ionised	
HES35	I13120-5453	13 15 06.3	-55 09 23	5.5	0.03076	molecular	
HES41	HB8905	05 07 36.4	+03 07 52	10.8	2.48	ionised	1ES 0414+009
HES48	I14378-3651	14 40 59.0	-37 04 32	7.1	0.06764	molecular	
HES48	IC4329A	13 49 19.2	-30 18 34	5.6	0.016054	UFO	
HES60	HE0109	01 11 43.5	-35 03 01	12.2	2.407	ionised	
HES64	MCG-5-23-16	09 47 40.1	-30 56 55	4.2	0.008486	UFO	
HES66	I08572+3915 ^b	09 00 25.4	+39 03 54	5.1	0.05835	molecular & ionised	
HES66	SDSSJ0745	07 45 21.8	+47 34 36	12.9	3.22	ionised	
HES66	SDSSJ0900 ^b	09 00 33.5	+42 15 47	6.3	3.297	ionised	
HES66	SMMJ0943 ^b	09 43 04.1	+47 00 16	15.2	3.351	ionised	
HES66	SDSSJ0841	08 41 30.8	+20 42 20	17.7	0.641	ionised	
HES66	SDSSJ0842	08 42 34.9	+36 25 03	2.4	0.561	ionised	
HES66	SDSSJ0858	08 58 29.6	+44 17 35	7.5	0.454	ionised	
HES66	SDSSJ0838	08 38 17.0	+29 55 27	8.4	2.043	BAL	
HES66	Mrk79	07 42 32.8	+49 48 35	14.8	0.022189	UFO	
HES66	APM08279	08 31 41.7	+52 45 18	14.5	3.91	UFO	
HES74	I23060+0505	23 08 33.9	+05 21 30	8.8	0.173	molecular	
HES79	SDSSJ0149	01 49 32.5	+00 48 04	10.7	0.567	ionised	
HES79	SDSSJ0210	02 10 47.0	-10 01 53	8.0	0.54	ionised	
HES79	Mrk279	00 52 08.9	-02 13 06	14.5	0.030451	warm absorber	
HES80	SDSSJ10100 ^c	10 10 43.4	+06 12 01	11.5	0.0984	ionised	
HES80	COS11363 ^c	10 00 28.7	+02 17 45	6.9	2.1	ionised	
HES80	XID2028 ^c	10 02 11.3	+01 37 07	6.5	1.593	ionised	
HES80	XID5321 ^c	10 03 08.8	+02 09 04	7.1	1.47	ionised	
HES80	XID5395 ^c	10 02 58.4	+02 10 14	7.1	1.472	ionised	
HES80	MIRO20581 ^c	10 00 00.6	+02 15 31	6.8	2.45	ionised	

^a Padovani et al. (2016)

^b also counterpart of ID 9

^c also counterpart of ID 11

per cent for $\text{FWHM}_{\text{Avg}} \gtrsim 800 \text{ km s}^{-1}$ for through-going ν_{μ} , which becomes ~ 22 per cent with the trial correction.

Figure 6 shows the chance probability of association of the SDSS sources with IceCube events for objects having $L_{[\text{O III}]}$ larger than the value on the x -axis. The dashed red line refers to cascades while the dotted blue line is for tracks; the solid orange line represents the full sample. The numbers give the observed (above the points) and average random value (below the points) of N_{ν} . Figure 6 shows the following:

(i) for both samples, but especially for tracks, the chance probability depends on power;

(ii) a p-value ~ 37 per cent is reached for $\log L_{[\text{O III}]} \gtrsim 40 \text{ erg s}^{-1}$ for tracks. This becomes ~ 48 per cent once the trial correction is applied;

(iii) a p-value ~ 72 per cent is reached for $\log L_{[\text{O III}]} \gtrsim 42.5 \text{ erg s}^{-1}$ for cascades. This becomes ~ 91 per cent once the trial correction is applied;

(iv) at the $\log L_{[\text{O III}]}$ at which the p-value for tracks is minimum N_{ν} is 21, while the average value from the ran-

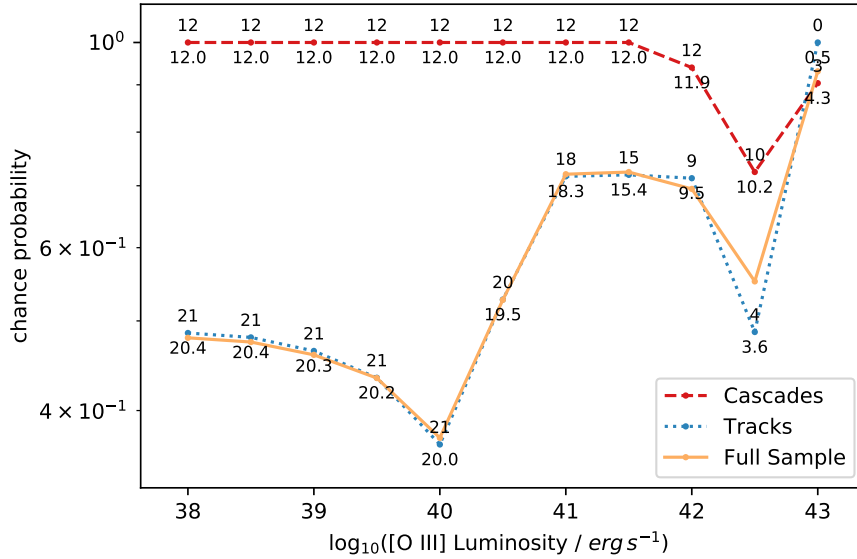


Figure 6. The chance probability of association of SDSS AGN for objects having $L_{[O III]}$ larger than the value on the x-axis with all IceCube events (solid orange line), cascades (dashed red line), and tracks (dotted blue line). The numbers give the observed (above the points) and average random values (below the points) of N_γ . A p-value ~ 37 per cent is reached for $\log L_{[O III]} \gtrsim 40 \text{ erg s}^{-1}$ for tracks.

domisation is 20.1, which means that only ≈ 1 IceCube track might have a “real” counterpart;

(v) for the same $\log L_{[O III]}$ the number of SDSS sources with a neutrino counterpart is 746, while the whole “parent” SDSS sample includes 22,153 sources;

(vi) the p-values for the full sample are, as expected, roughly in between those for cascades and tracks.

If we split the tracks even further we get a p-value ~ 18 per cent for $\log L_{[O III]} \gtrsim 41.5 \text{ erg s}^{-1}$ for HESE tracks, which becomes ~ 39 per cent with the trial correction.

In summary, our statistical analysis shows no significant results, although our best results are intriguing. We find in fact a p-value ~ 6 per cent for $\text{FWHM}_{\text{Avg}} \gtrsim 800 \text{ km s}^{-1}$ for through-going ν_μ (~ 22 per cent post-trial) and ~ 18 per cent for $\log L_{[O III]} \gtrsim 41.5 \text{ erg s}^{-1}$ for HESE tracks (~ 39 per cent post-trial).

4 ASTROPHYSICAL INTERPRETATION

Our main result is that AGN with “bona fide” outflows associated with an IceCube neutrino have \dot{E}_{kin} , \dot{M}_{OF} , and bolometric power larger than those of AGN with outflows not matched to neutrinos (by factors $\sim 4 - 7$). The corresponding distributions are different for the two classes of AGN at the $\gtrsim 99.6$ per cent level for the first two parameters and at the $\gtrsim 96.2$ per cent level for the third one. This makes perfect astrophysical sense, since AGN with larger outflow and kinetic energy rates and bolometric powers are also likely to be stronger neutrino emitters (e.g., Wang & Loeb 2016).

One could argue that some of the presumed associations in Tab. 2 are not very realistic, as there are more plausible HBL counterparts. This could certainly be the case, but it is hard to be more quantitative about this as Padovani et al. (2016) find a chance probability of association with HBL

only at the ~ 1.4 per cent level (2.2σ : Resconi et al. 2017). A similar analysis cannot be applied to the AGN outflow list since, although it is a very comprehensive compilation, it does not represent a well-defined, complete sample.

We have then carried out a statistical analysis on the SDSS AGN catalogue, finding no direct evidence of an association with the IceCube events. However: (1) the value of the FWHM_{Avg} for which we get the smallest p-value for tracks ($\gtrsim 800 \text{ km s}^{-1}$) is very interesting from the astrophysical point of view, as it is above the limit normally used to select targets for follow-up studies of AGN outflows (500 km s^{-1}); (2) through-going ν_μ alone provide a small excess ($\sim 2\sigma$ pre-trial), which we interpret as a fluctuation but goes in the right direction at an astrophysically relevant FWHM_{Avg} ; (3) HESE tracks alone give a p-value ~ 18 per cent for $\log L_{[O III]} \gtrsim 41.5 \text{ erg s}^{-1}$ (which becomes ~ 39 per cent with the trial correction), which is an astrophysically interesting value as, by selecting the upper ~ 22 per cent of the $L_{[O III]}$ distribution, it points to relatively powerful AGN, which are the most likely outflow candidates; (4) only a small fraction of the high FWHM_{Avg} AGN in the SDSS catalogue are confirmed outflow sources (Harrison et al. 2014), the majority being still *potential* outflows; (5) finally, it could also be that FWHM_{Avg} is a poor proxy for outflow power, unlike \dot{E}_{kin} and \dot{M}_{OF} , which depend also on the mass and the radius involved ($\dot{E}_{\text{kin}} = \frac{1}{2} \dot{M}_{\text{OF}} v_{\text{max}}^2$ and $\dot{M}_{\text{OF}} = 3 \times v_{\text{max}} \times \dot{M}_{\text{OF}} / R_{\text{OF}}$: see eq. B.2 of Fiore et al. 2017). That could also explain the differences between the results derived from the two approaches.

Our results have two possible implications:

(i) AGN outflows are neutrino emitters but at present we cannot get a significant signal from them. This could be because the neutrino and “bona fide” outflow statistics are still too low or AGN outflows are so faint that they cannot be revealed as point sources but contribute to the background

neutrino emission. This would explain both the results from the AGN outflow list and those from the SDSS catalogue. In this case AGN outflows appear to be able to explain only up to ~ 6 per cent of the IceCube signal;

(ii) AGN outflows are not neutrino sources.

Based on our results, we believe implication (ii) is not the most favoured one at present. Further progress on this topic requires: (1) better neutrino statistics, which will come with time as IceCube keeps taking data. Unfortunately, the event rate is not very high (of the order of 15 yr^{-1}); (2) stacking at the positions of the outflows. This can be carried out by the IceCube consortium as done, for example, for blazars by [IceCube Collaboration \(2017c\)](#); (3) a complete catalogue of AGN outflows. The main limitation of our work, in fact, is that we either have a list of certified outflows, which however is not a well-defined, complete sample or we have a catalogue of mostly *potential* sources. Ideally one would like to have a well-defined, complete catalogue of “bona fide” AGN outflows, but this is not available at present.

We stress that our results do not appear to support a scenario where AGN outflows explain the *whole* IceCube signal, as suggested by [Wang & Loeb \(2016\)](#) and [Lamastra et al. \(2017\)](#), but instead might corroborate the work of [Liu et al. \(2018\)](#), who predict a smaller contribution.

5 CONCLUSIONS

We have directly tested for the first time the existence of a new class of neutrino sources, namely matter outflows associated with AGN. We have first cross-correlated a list of 94 “bona fide” AGN outflows put together by [Fiore et al. \(2017\)](#) with the only complete and updated repository of IceCube neutrinos currently publicly available, collected by us for this purpose. Our main result is that AGN with outflows associated with an IceCube neutrino have outflow and kinetic energy rates and bolometric powers larger than those of AGN with outflows not matched to neutrinos. The corresponding distributions are also different for the two AGN classes, significantly so for the first two parameters ($\gtrsim 99.6$ per cent). A proper statistical analysis of this association cannot be carried out since the AGN outflow list, although very comprehensive, does not represent a well-defined, complete sample.

We have then carried out a statistical analysis on a catalogue of [O III] $\lambda 5007$ line profiles using a sample of 23,264 SDSS AGN at $z < 0.4$ ([Mullaney et al. 2013](#)), which can be used to determine the kinematics of the kpc-scale emitting gas. One can use the [O III] $\lambda 5007$ flux-weighted average FWHM as a proxy to select AGN with potential outflows, together with $L_{[\text{O III}]}$. We find no significant evidence of an association between the SDSS AGN and the IceCube events, although the values of FWHM_{Avg} and $\log L_{[\text{O III}]}$ for which we get the smallest p-values (~ 6 and 18 per cent respectively, pre-trial) make perfect astrophysical sense. The former, in particular ($\text{FWHM}_{\text{Avg}} \gtrsim 800 \text{ km s}^{-1}$), is above the limit normally used to select targets for follow-up studies of AGN outflows (500 km s^{-1}).

Our results are consistent with a scenario where AGN outflows are neutrino emitters but at present do not provide a significant signal. This can be tested with better outflow and neutrino statistics and stacking. In any case, we appear

to rule out a predominant role of AGN outflows in explaining the IceCube data.

ACKNOWLEDGMENTS

We thank Chris Harrison and Vincenzo Mainieri for useful suggestions and discussions, Fabrizio Fiore for sending us the coordinates of the sources in Tab. B1 of [Fiore et al. \(2017\)](#), Stefan Coenders for his contribution to the statistical analysis and the teams, which have produced the data and catalogues used in this paper for making this work possible. ER is supported by a Heisenberg Professorship of the Deutsche Forschungsgemeinschaft (DFG RE 2262/4-1). This work was supported by the Deutsche Forschungsgemeinschaft through grant SFB 1258 “Neutrinos and Dark Matter in Astro- and Particle Physics”. We made use of the TOPCAT ([Taylor 2005](#)) and of the R ([R Core Team 2017](#)) software packages.

REFERENCES

- Aartsen M. G., et al., 2013, *Phys. Rev. Lett.*, 111, 021103
Aartsen M. G., et al., 2015, *Phys. Rev. Lett.*, 115, 081102
Aartsen M. G., et al., 2016, *ApJ*, 833, 3
Aartsen M. G., et al., 2017, *ApJ*, 835, 45
Ackermann M., et al., 2016, *ApJS*, 222, 5
Ahlers M., Halzen F., 2015, *Rep. Prog. Phys.*, 78, 126901
Emig K., Lunardini C., Windhorst R., 2015, *JCAP*, 12, 029
Fabian A. C., 2012, *ARA&A*, 50, 455
Fiore F., et al., 2017, *A&A*, 601, A143
Giommi P., Padovani P., Polenta G., Turriziani S., D’Elia V., Piranomonte S., 2012, *MNRAS*, 420, 2899
Halzen F., Zas E., 1997, *ApJ*, 488, 669
Harrison, C. M., Alexander, D. M., Mullaney, J. R., & Swinbank, A. M. 2014, *MNRAS*, 441, 3306
Harrison C. M., 2017, *NatAs*, 1, 0165
IceCube Collaboration, 2013, *Science*, 342, 1242856
IceCube Collaboration, 2014, *Phys. Rev. Lett.*, 113, 101101
IceCube Collaboration, 2015a, Contributions to the 34th International Cosmic Ray Conference (ICRC 2015), p. 45 (arXiv:1510.05223)
IceCube Collaboration, 2015b, Contributions to the 34th International Cosmic Ray Conference (ICRC 2015), p. 37 (arXiv:1510.05223)
IceCube Collaboration, 2017a, Contributions to the 35th International Cosmic Ray Conference (ICRC 2017), p. 30 (arXiv:1710.01191)
IceCube Collaboration, 2017b, Contributions to the 35th International Cosmic Ray Conference (ICRC 2017), p. 54 (arXiv:1710.01191)
IceCube Collaboration, 2017c, Contributions to the 35th International Cosmic Ray Conference (ICRC 2017), p. 31 (arXiv:1710.01179)
King A., Pounds K., 2015, *ARA&A*, 53, 115
Kopper C., Blaufuss E., 2017, *GCN.2*, 21916, 1
Lamastra A., Menci N., Fiore F., Antonelli L. A., Colafrancesco S., Guetta D., Stamerra A., 2017, *A&A*, 607, A18
Liu R.-Y., Murase K., Inoue S., Ge C., Wang X.-Y., 2018, *ApJ*, submitted (arXiv:1712.10168)
Lucarelli F., et al., 2017a, *ApJ*, 846, 121
Lucarelli F., et al., 2017b, *ATel*, 10801
Mannheim K., 1995, *Astroparticle Physics*, 3, 295
Mirzoyan R., 2017, *ATel*, 10817
Mücke A. et al., 2003, *Astroparticle Physics*, 18, 593

- Mullaney J. R., Alexander D. M., Fine S., Goulding A. D., Harrison C. M., Hickox R. C., 2013, *MNRAS*, 433, 622
- Padovani P., Giommi P., 1995, *ApJ*, 444, 567
- Padovani P., Resconi E., 2014, *MNRAS*, 443, 474 (PR14)
- Padovani P., Petropoulou M., Giommi P., Resconi E., 2015, *MNRAS*, 452, 1877
- Padovani P., Resconi E., Giommi P., Arsioli B., Chang Y. L., 2016, *MNRAS*, 457, 3582
- Padovani P., et al., 2017, *A&ARv*, 25, 2
- Palladino A., Vissani F., 2017, *A&A*, 604, A18
- Patrignani C., Particle Data Group, 2016, *ChPhC*, 40, 100001, p. 528
- Petropoulou M., Dimitrakoudis S., Padovani P., Mastichiadis A., Resconi E., 2015, *MNRAS*, 448, 2412
- R Core Team, 2017, R Foundation for Statistical Computing
<https://www.R-project.org/>
- Resconi E., Coenders S., Padovani P., Giommi P., Caccianiga L., 2017, *MNRAS*, 468, 597
- Tanaka Y. T., Buson S., Kocevski D., 2017, *ATel*, 10791
- Tavecchio F., Ghisellini G., 2015, *MNRAS*, 451, 1502
- Taylor M. B. 2005, *Astronomical Data Analysis Software and Systems XIV*, 347, 29
- Urry C. M., Padovani P., 1995, *PASP*, 107, 803
- Wang X., Loeb A., 2016, *JCAP*, 12, 012

This paper has been typeset from a $\text{\TeX/L}^{\text{A}}\text{\TeX}$ file prepared by the author.